

SIMULATIONS OF INTERLAYER METHANOL IN Ca- AND Na-SATURATED MONTMORILLONITES USING MOLECULAR DYNAMICS

MARCO PINTORE¹, SALVATORE DEIANA², PIERFRANCO DEMONTIS³, BRUNO MANUNZA², GIUSEPPE BALDOVINO SUFFRITTI³ AND CARLO GESSA⁴

¹ Laboratory of Chemometrics & BioInformatics, University of Orléans, B.P. 6759, 45067 Orléans Cedex 2, France

² Dipartimento di Scienze Ambientali Agrarie e Biotecnologiche Agroalimentari, Università di Sassari, V. le Italia 39, I-07100 Sassari, Italy

³ Dipartimento di Chimica, Università di Sassari, Via Vienna 2, I-07100 Sassari, Italy

⁴ Istituto di Chimica Agraria, Università di Bologna, V. le Bertini-Pichat 10, I-40127 Bologna, Italy

Abstract—Molecular dynamics computer simulations were used to study methanol molecules confined between the layers of 2:1 phyllosilicates. The model systems are based on natural Ca- and Na-rich montmorillonites. Data from the literature and determined by fitting the calculated layer spacing to experimental values were employed to obtain interactions between the charged 2:1 layers and the solvent molecules. The montmorillonite surface atoms were held rigid and the methyl group in the methanol molecule was represented by a soft Lennard-Jones sphere. Electrostatic interactions were determined by the Ewald sum method, whereas the van der Waals interactions were described by a Lennard-Jones potential. Comparison of our results with diffraction data indicates a good reproduction of the layer spacing. After the initial solvent layer forms, additional solvent layers form only after previous layers are complete. Each Ca²⁺ and Na⁺ ion in the monolayer has four and two methanol molecules, respectively, in the first solvation shell, whereas the solvation shell in the multilayer contains six and four methanol molecules, respectively. This agrees well with experimental data.

Key Words—Methanol, Molecular Dynamics, Montmorillonite.

INTRODUCTION

Clay minerals and their interactions with a wide range of solvents or intercalate molecules have been investigated using several experimental techniques, such as X-ray diffraction (XRD) (Lanson, 1997), nuclear magnetic resonance (NMR) (Grandjean and Laszlo, 1989), infrared (IR) (Sposito and Prost, 1982), ultraviolet (UV) (Villemure *et al.*, 1986) and electron paramagnetic resonance (EPR) (Boyd and Mortland, 1985) spectroscopies, and thermal and calorimetric analysis (Mackenzie and Mitchell, 1972). A satisfactory interpretation of all the collected data requires a complete description, on the atomic scale, of the interactions between the aluminosilicate framework, the solvent molecules, and the exchangeable ions. Recently, computational techniques such as Monte Carlo (Delville, 1993; Skipper *et al.*, 1995) and molecular dynamics (Keldsen *et al.*, 1994; Chang *et al.*, 1995) were helpful in the analysis of adsorption of H₂O molecules in the interlayer, providing a good description of their organization around the counterions and allowing the computation of diffusion coefficients. Until now, computational studies on the adsorption of organic molecules have focused on the adsorption enthalpy of aliphatic chains (Keldsen *et al.*, 1994) or the configurational analysis of more complex structures (Sato *et al.*, 1996), neglecting the disorder state of the interlayer species.

In this work, we used molecular dynamics calculations to study the arrangement of methanol molecules at different concentrations in Ca- and Na-saturated montmorillonites. We chose methanol for the following reasons: (1) the relative simplicity of the methanol structure allows us to use affordable computational facilities; (2) methanol molecules are analogous to the H₂O molecule whose behavior in clays has been studied extensively; (3) the research may be extended to the study of molecular dynamics of ethylene glycol, a compound used for the experimental determination of the surface area of clays (Eltantawy and Arnold, 1974).

MATERIALS AND METHODS

A montmorillonite from Camp Berteau was chosen as the model phyllosilicate for this study because of the availability of adsorption data (Annabi-Bergaya *et al.*, 1979, 1980a,b, 1981). The unit-cell formula, inferred from chemical composition data (van Olphen and Fripiat, 1979) and adjusted slightly for modeling requirements, is $M^{n+}_{1.0n}[\text{Si}_{7.875}\text{Al}_{0.125}](\text{Al}_{2.875}\text{Fe}_{0.25}\text{Mg}_{0.875})\text{O}_{20}(\text{OH})_4$, where $M^{n+} = \text{Ca}^{2+}$ or Na^{+} . The selected simulation cell contains one $20.68 \times 17.90 \text{ \AA}^2$ slab of a 2:1 layer (eight unit-cells); periodic boundary conditions were applied along the three dimensions to reproduce a stack of layers. The effective charges assigned to the framework atoms (Table 1) were adopted from Skipper *et al.* (1995). To replace an ^{VI}Al by

Table 1. Atomic positions and effective charges Q in the unit-cell of the collapsed structure of a montmorillonite 2:1 layer (orthogonal cell; $a = 5.17 \text{ \AA}$, $b = 8.95 \text{ \AA}$, $c = 6.60 \text{ \AA}$).

Atom	$x(\text{\AA})$	$y(\text{\AA})$	$z(\text{\AA})$	Q (evu)	Atom	$x(\text{\AA})$	$y(\text{\AA})$	$z(\text{\AA})$	Q (evu)
O	0.511	0.000	0.333	-0.8	Al	1.362	0.680	0.000	3.0
O	0.255	0.256	0.333	-0.8	Al	1.362	0.341	0.000	3.0
O	0.766	0.256	0.333	-0.8	O	0.170	1.020	-0.333	-0.8
O	0.000	0.000	0.108	-1.7	O	0.426	0.766	-0.333	-0.8
H	0.171	0.000	0.146	0.7	O	-0.085	0.766	-0.333	-0.8
Si	0.511	0.170	0.277	1.2	O	0.681	1.020	-0.108	-1.7
Si	0.000	0.341	0.277	1.2	H	0.510	1.020	-0.146	0.7
O	0.511	0.170	0.108	-1.0	Si	0.171	0.851	-0.277	1.2
O	0.000	0.341	0.108	-1.0	Si	0.681	0.765	-0.277	1.2
Al	0.851	0.170	0.000	3.0	O	0.170	0.851	-0.108	-1.0
Al	0.851	-0.170	0.000	3.0	O	0.681	0.680	-0.108	-1.0
O	0.000	0.511	0.333	-0.8	O	0.681	0.511	-0.333	-0.8
O	0.766	0.765	0.333	-0.8	O	-0.085	0.256	-0.333	-0.8
O	0.255	0.765	0.333	-0.8	O	0.426	0.256	-0.333	-0.8
O	0.511	0.511	0.108	-1.7	O	0.170	0.511	-0.108	-1.7
H	0.681	0.511	0.146	0.7	H	0.000	0.511	-0.146	0.7
Si	0.000	0.680	0.277	1.2	Si	0.681	0.341	-0.277	1.2
Si	0.511	0.851	0.277	1.2	Si	0.171	0.170	-0.277	1.2
O	0.000	0.680	0.108	-1.0	O	0.681	0.341	-0.108	-1.0
O	0.511	0.851	0.108	-1.0	O	0.170	0.170	-0.108	-1.0

Mg and a Si by ^{IV}Al , we reduced the charges on these sites from 3 electrostatic valency units (evu) to 2 evu and from 1.2 evu to 0.2 evu, respectively. Molecular dynamics simulations were performed using the DL-POLY-2.0 molecular dynamics program (Smith and Forester, 1996). The surface atoms were held rigid. A flexible substrate was recently found experimentally in phyllosilicates (Vahedi-Faridi and Guggenheim, 1999), although earlier work on zeolites and framework structures did not suggest a need for a flexible substrate. Thus, although a rigid framework was used in this work, future studies will need to consider a flexible substrate in phyllosilicates. Based on the results of Vahedi-Faridi and Guggenheim (1999), the formal charges as presented by Skipper *et al.* (1995) should be reconsidered.

The methanol molecules and the cations neutralizing the negative layer charge were left unconstrained. The methyl group of the methanol molecule was represented by a soft Lennard-Jones sphere. Skipper *et al.* (1995) showed that, even for small simulation cells, the computed properties are representative of the macroscopic system and are not influenced by the artificial long-range symmetry of the imposed periodic lattice. We apply a cut-off of 8.95 \AA for the short-range contributions to the potential energy, thereby treating the interactions within an all-image regime (Allen and Tildesley, 1987).

The intermolecular potential function that accounts for the interactions in our model is:

$$U(r_{ij}) = \sum_i \sum_{j>i} \left[\frac{q_i q_j}{r_{ij}} + \frac{A_{ij}}{r_{ij}^{12}} - \frac{B_{ij}}{r_{ij}^6} \right] \quad (1)$$

where the indices i and j refer to all the sites of each

molecule, q_i is the effective charge on the i^{th} site, r_{ij} is the intermolecular separation, and A_{ij} and B_{ij} represent two variable parameters accounting for the interactions between the i^{th} and j^{th} sites. The following interactions were considered (Table 2): cation-cation, cation-montmorillonite, cation-methanol, montmorillonite-montmorillonite, montmorillonite-methanol and methanol-methanol.

The H1 model (Haughney *et al.*, 1987; Ferrario *et al.*, 1990) was used to describe the methanol-methanol interactions and treats the methanol molecule as a rigid structure whose interaction centers are located on the C atom, the O nucleus, and the OH proton. A charge of -0.728 evu is assigned to the O atom and balancing charges of 0.297 evu and 0.431 evu are assigned to the CH_3 group and OH proton, respectively. Lennard-Jones terms account for the van der Waals interactions. The interactions between the interlayer species (methanol and Ca^{2+} or Na^+ ions) and the framework atoms are represented by Coulomb forces and by Lennard-Jones potential functions. The parameters included in the functions were obtained from the Universal Force Field scheme (Rappé *et al.*, 1992), adequately modified to represent both the pressure of 0.1 MPa and the experimental values of the interlayer spacing (Annabi-Bergaya *et al.*, 1979) at a methanol content of 2.5, 3.4, 4.2 and 5.0 mmol per g of Ca-clay, and 0.85, 1.85 and 2.01 mmol per g of Na-clay. The montmorillonite-montmorillonite interactions and those concerning the H atoms were modeled only by Coulomb forces and not using the Lennard-Jones terms.

Long-range electrostatic interactions were calculated by using the Ewald sum technique (Allen and Tildesley, 1987). We used a convergence parameter $\mathbf{k} =$

Table 2. Parameters in the potential function.

Sites	$A_{ij} \times 10^{-6}$ (kcal Å ¹² /mol)	$B_{ij} \times 10^{-3}$ (kcal Å ⁶ /mol)
Methanol-methanol		
CH ₃ -CH ₃	7.947	2.399
CH ₃ -O	2.183	1.246
O-O	0.515	0.600
Methanol-counterion		
CH ₃ -Ca	0.814	0.717
O-Ca	0.338	0.401
CH ₃ -Na	0.342	1.858
O-Na	0.355	6.600
Methanol-montmorillonite		
CH ₃ -Al	6.451	2.436
CH ₃ -Si	4.273	1.871
CH ₃ -Mg	0.293	0.355
CH ₃ -Fe	0.828	0.111
CH ₃ -O	0.413	0.542
O-Al	2.919	1.425
O-Si	1.907	1.087
O-Mg	0.119	0.197
O-Fe	0.330	0.061
O-O	0.407	0.533
Counterion-montmorillonite		
Ca-Al	4.991	0.172
Ca-Si	3.247	0.080
Ca-Mg	0.195	0.009
Ca-Fe	0.547	0.111
Ca-O	0.968	0.051
Ca-Ca	0.666	0.074
Na-Al	0.924	0.374
Na-Si	0.593	0.211
Na-Mg	0.131	0.084
Na-Fe	0.085	0.045
Na-O	0.656	0.098
Na-Na	0.065	0.042

0.36 Å⁻¹, including all vectors $\mathbf{k} < 8 \text{ Å}^{-1}$, 7 Å^{-1} and 6 Å^{-1} (along three axis directions, respectively) in the reciprocal space sum and all $r_{ij} < 8.95 \text{ Å}$ in the real space sum.

Self-diffusion coefficients (D) for the motion of either methanol molecules or exchangeable ions within

the interlayer were estimated using the two-dimensional Einstein relation

$$D = \lim_{t \rightarrow \infty} \frac{1}{4} \frac{d}{dt} \langle r^2 \rangle \quad (2)$$

where $\langle r^2 \rangle$ is the mean-square displacement (MSD) and t is time.

All simulations were conducted at 300 K. To simulate the transition between the monolayer and the multilayer structures, the number of methanol molecules in the interlayer was varied from 15 to 65 (2.5–10.9 mmol/g) and from 5 to 35 (0.85–5.85 mmol/g) for the Ca- and the Na-rich montmorillonite, respectively. All dynamics consisted of an initial run in the canonical ensemble NVT (where the particle numbers N , the volume V , and the temperature T are fixed) of 50,000 steps (using 1×10^{-15} s per step) and an expansion run in the ensemble $N\sigma T$ (where the particle numbers N , the normal stress σ and the temperature T are fixed) of 2,000,000 steps, to obtain reliable values of the diffusion coefficients; the value of σ was set at 0.1 Mpa. The energy of the systems was always conserved. The interlayer spacing, the radial distribution functions, and the orientations of methanol molecules in the phyllosilicate were calculated from the data collected in the last 50,000 steps. The calculations were executed on an IBM RS 6000/3CT workstation.

RESULTS AND DISCUSSION

Ca-exchanged montmorillonite

The calculated and experimental layer-spacing values vs. methanol content are given in Table 3. The good fit of the calculated interlayer spacings to the experimental data is related to the parametrization of the force field. The structure of the adsorbed methanol molecules was obtained by evaluating the mean radial distribution functions $[g(r)]$ between the solvent molecules, the Ca²⁺ ions and the framework atoms, and by determining the instantaneous equilibrium configurations of the methanol molecules.

Table 3. Comparison between experimental and computed layer spacing for the Ca-clay and Na-clay system. The uncertainties were derived by applying a root-mean-square procedure to the deviations obtained at equilibrium. Experimental uncertainties are not available.

Ca-clay			Na-clay		
Methanol content (mmol/g)	Layer spacing (Å) (experimental)	Layer spacing (Å) (computed)	Methanol content (mmol/g)	Layer spacing (Å) (experimental)	Layer spacing (Å) (computed)
2.50	13.30	13.20 ± 0.09	0.00	9.70	9.71 ± 0.08
3.40	14.30	14.30 ± 0.10	0.85	9.70	11.53 ± 0.08
4.20	15.20	15.30 ± 0.12	1.85	12.70	12.75 ± 0.10
5.00	16.50	16.40 ± 0.15	2.01	13.00	13.09 ± 0.13
5.90		18.30 ± 0.20	2.70		13.96 ± 0.14
6.70		19.25 ± 0.20	3.35		14.25 ± 0.18
7.50		20.20 ± 0.25	4.19		14.92 ± 0.25
8.00		21.40 ± 0.33	5.02		16.06 ± 0.30
10.90		24.75 ± 0.40	5.85		17.23 ± 0.32

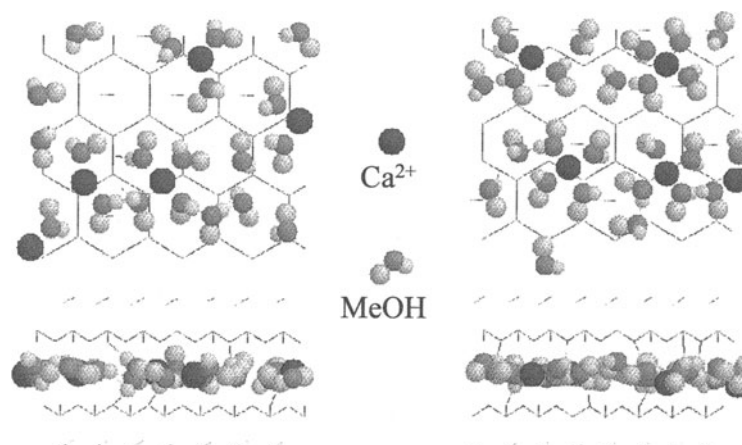


Figure 1. Top (upper) and lateral (lower) 'snapshots' showing the distribution of methanol molecules in the interlayer of Ca-rich montmorillonite with a solvent content of 3.4 (left) and 4.2 (right) mmol/g. The Me symbol denotes the methyl group.

The arrangement of the methanol molecules in the interlayer for a solvent content of 3.4 and 4.2 mmol/g is shown in Figure 1. The solvent molecules form a hydrogen bond network and occupy a monolayer film around the Ca^{2+} ions, towards which the methanol oxygen atoms point. The layer coverage is complete where the methanol content reaches 4.2 mmol/g. Complete filling of the first layer is required before the second layer starts to form. This behavior does not agree with experimental data (Pamar-Robert *et al.*, 1989) that provides evidence for interstratification phenomena; the disagreement may be related either to errors in the model or to residual H_2O present in the natural montmorillonite, which may affect the methanol arrangement in the layers.

Figures 2 shows 'snapshots' illustrating the filling of the second layer and the initial stage of the third

layer. The transition between bi-layer and triple-layer is emphasized in Table 3, where regular increasing of the layer spacing changes abruptly at 5.0 mmol/g (shift from the first to the second layer) and at 7.5 mmol/g (shift from the second to the third layer). The transition concentrations agree well with the data from Robert-Pamar *et al.* (1989), where the presence of the monolayer, the bi-layer and the triple-layer are associated with methanol contents of 3.1–3.5, 6.3–7.0 and 9.3–10.5 mmol/g, respectively.

The upper part of Figure 3 shows the dependence of the $g(r)$ functions between the methanol O atoms and the Ca^{2+} ions on the methanol concentration. The first peak, due to the first solvation shell, shifts from 2.2 to 2.5 Å as the second layer fills. The shift is related to increased cohesion of the solvent molecules

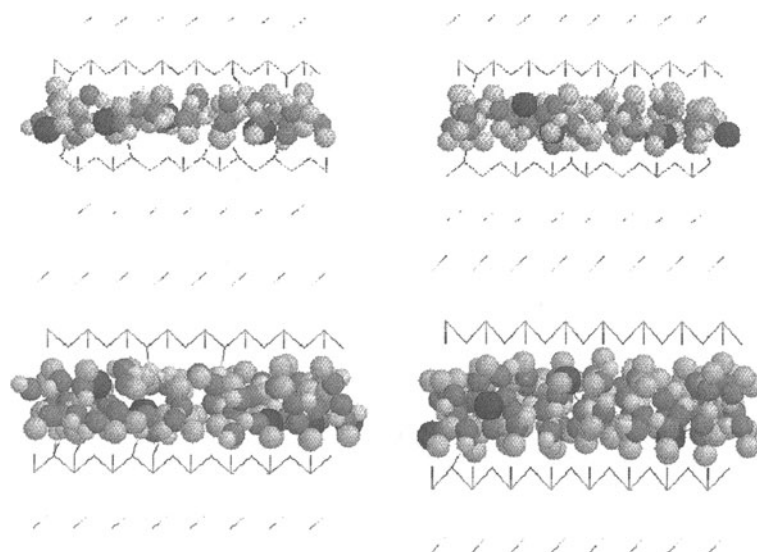


Figure 2. Lateral 'snapshots' showing the distribution of methanol molecules in the interlayer of Ca-rich montmorillonite with a solvent content of 5.9 (upper, left), 6.7 (upper, right), 8.4 (lower, left), and 10.9 (lower, right) mmol/g.

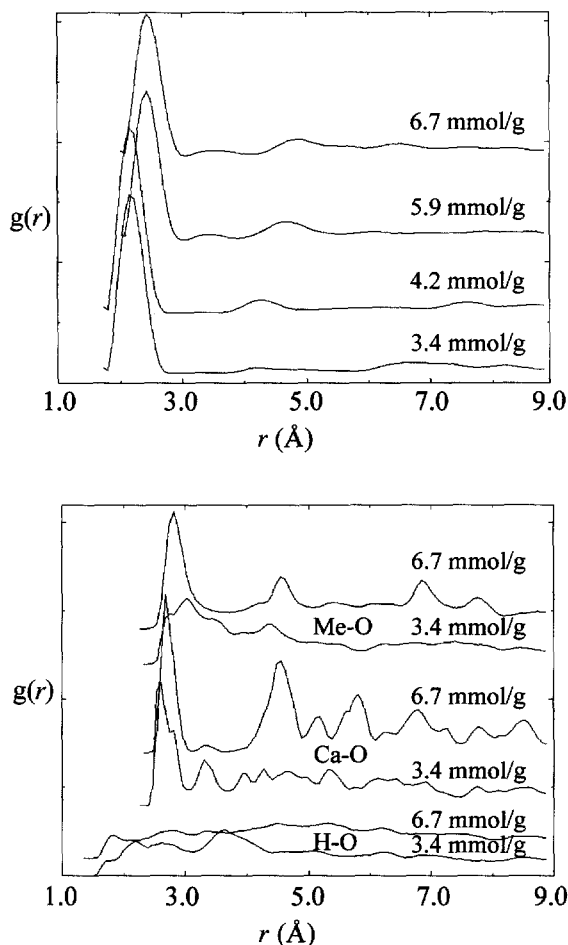


Figure 3. (Upper) Ca-O radial distribution functions $g(r)$ for solvent contents of 3.4, 4.2, 5.9 and 6.7 mmol/g. O denotes the oxygen atom of the methanol. (Lower) H-O, Ca-O, and Me-O $g(r)$ functions for solvent contents of 3.4 and 6.7 mmol/g. O, Me and H represent the oxygen atoms of the framework, the methyl groups, and the hydrogen atoms of the methanol molecule, respectively. All of the $g(r)$ functions were evaluated by averaging the configurations related to the final 50,000 steps of the expansion run in the ensemble $N\sigma T$.

as the second layer fills and the consequent lowering of the strength of the calcium-methanol interaction.

The Ca-O, Me-O and H-O $g(r)$ functions (O, Me and H denote the oxygen atoms of the framework, the methyl groups, and the hydrogen atoms of the methanol molecule, respectively) are shown in the lower part of Figure 3 for two different methanol concentrations, 3.4 and 6.7 mmol/g, representative of the mono- and the bi-layer configurations. For simplicity, we do not report the $g(r)$ functions between the O atoms of the methanol and the framework, as those are similar to the Me-O distribution functions. The bi-layer system exhibits a more ordered distribution of solvent molecules than the monolayer system: the patterns of the $g(r)$ functions for the monolayer and bi-layer sys-

Table 4. Self-diffusion coefficients (D) of interlayer methanol molecules and metal counterions at $T = 289$ K. The uncertainties were derived by the analysis of the residuals obtained from the Einstein equation.

Ca-rich montmorillonite		
Methanol content (mmol/g)	$D(\text{Ca}^{2+}) \times 10^{12}$ (m^2/s)	$D(\text{CH}_3\text{OH}) \times 10^{12}$ (m^2/s)
3.40	4.5 ± 0.4	7.8 ± 0.5
4.20	1.9 ± 0.3	5.1 ± 0.4
5.90	0.3 ± 0.2	0.7 ± 0.3
6.70	0.2 ± 0.3	0.6 ± 0.2
Na-rich montmorillonite		
Methanol content (mmol/g)	$D(\text{Na}^+) \times 10^{12}$ (m^2/s)	$D(\text{CH}_3\text{OH}) \times 10^{12}$ (m^2/s)
2.01	2.1 ± 0.3	8.2 ± 0.3
3.35	58 ± 5	210 ± 14
4.19	260 ± 12	650 ± 21

tems are typical of a crystalline solid and a viscous liquid, respectively. These distributions agree with the slow diffusion of Ca^{2+} ions and of methanol as determined by computation (Table 4). The diffusion coefficients for the configurations represented in the lower part of Figure 3 differ by a factor of 10, indicating that the interlayer species in the bi-layer system are nearly rigid. The slow diffusion of methanol molecules is attributed to the formation of H bridges and strong van der Waals interactions between solvent molecules, Ca^{2+} ions and the framework, as indicated by the sharp peaks in the range from 2.0 to 3.0 Å.

Figure 4 shows the dependence of the solvation number of Na^+ and Ca^{2+} on the solvent content. The solvation number of Ca^{2+} varies from 2 to 4 in the monolayer, and increases to 6 as the bi-layer fills. Annabi-Bergaya *et al.* (1981) reported a maximum coordination number of 4 for a methanol content of 5.0 mmol/g and attributed it to the complete formation

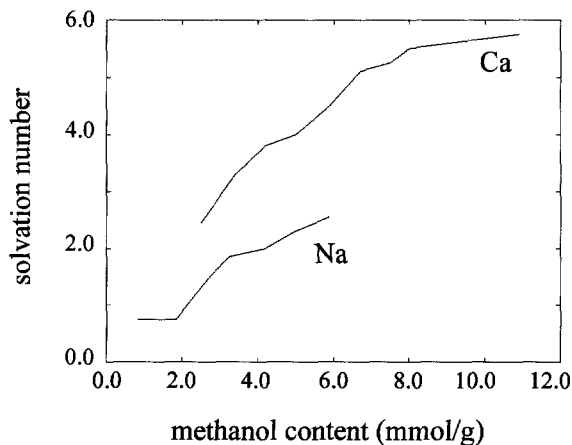


Figure 4. Relationship between the Ca^{2+} and Na^+ solvation number, and the methanol content.

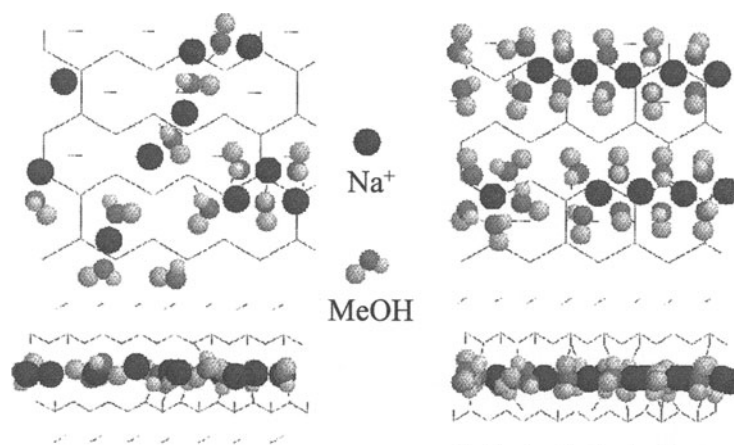


Figure 5. Top (upper) and lateral (lower) 'snapshots' showing the distribution of methanol molecules in the interlayer of Na-rich montmorillonite for solvent contents of 2.01 (left) and 4.19 (right) mmol/g. The Me symbol denotes the methyl group.

of a bi-layer. According to our results, a 5.0 mmol/g concentration occurs as the second layer starts filling and the computed coordination number is 4.35.

Na-exchanged montmorillonite

The calculated and experimental values of the interlayer spacing are reported in Table 3. Apart from the methanol concentration of 0.85 mmol/g, the agreement between the calculated and experimental data is good. Note that the experimental results report the same layer spacing at 0.00 and 0.85 mmol/g, and this, obviously, is not reproducible with the technique employed.

Figure 5 shows a typical equilibrium configuration of the systems at concentrations of 2.01 and 4.19 mmol/g, where the filling process is complete. The solvent molecules are organized in a monolayer and form clusters around the Na⁺ ions. The linear arrangement of the metal ions, bridged by the methanol molecules, agrees well with reports concerning montmorillonites saturated with monovalent cations (Annabi-Bergaya *et al.*, 1981). The bi-layer formation starts between 4.19–5.02 mmol/g. The Na⁺ solvation number *vs.* the methanol content relationship is reported in Figure 4; the maximum solvation number for a monolayer is 2 and this value increases to 4 during the formation of the bi-layer system. These findings are consistent with the experimental data of Annabi-Bergaya *et al.* (1981), who found that the maximum methanol content in a monolayer Na-rich montmorillonite is 2.00–2.10 mmol/g, corresponding to a coordination number of 1.

The upper part of Figure 6 shows the *g(r)* functions for Na-O interactions in the Na-rich systems with methanol contents of 2.01, 4.19 and 5.02 mmol/g. The curves show one peak at 2.2 Å, due to the first solvation shell. The peak does not shift to larger distances

as the second layer fills, thus differing from the behavior of Ca-rich montmorillonite.

The Na-O, Me-O and H-O *g(r)* functions for the Na-rich systems are shown in the lower part of Figure 6 for methanol contents of 2.01 and 4.19 mmol/g. The arrangement of methanol molecules does not change significantly when bi-layer formation starts while the solvation and the mobility of the Na⁺ ions increase. This increase is indicated by the peaks of the Na-O *g(r)* function which broaden as the layer fills. The self-diffusion coefficients reported in Table 4 also confirm this trend: the values relative to these concentrations differ by a factor 10².

Adsorption energies

Experimental studies (Annabi-Bergaya *et al.*, 1979, 1980a; Robert-Pamar *et al.*, 1989) showed that the methanol insertion capacity agrees with one inserted layer for Na-rich montmorillonite and two inserted layers for Ca-rich montmorillonite. The use of molecular dynamics calculations to compute adsorption isotherms requires simulations performed at fixed chemical potential and variable particle numbers. This is very demanding for molecular dynamics techniques and we performed all computations in the *NVT* and *NσT* ensembles. We analyzed the internal energies (*U*) of the various systems at the end of the simulations. The variation in the internal energy of the interlayer methanol, Δ*U*(*c*), *vs.* the methanol content is reported in Figure 7, in which

$$\Delta U(c) = \frac{U(c) - U(0)}{N} \quad (3)$$

where *c* is the methanol content and *N* is the number of methanol molecules in the interlayer.

For either Na-rich montmorillonite or Ca-rich montmorillonite systems, the adsorption of methanol mol-

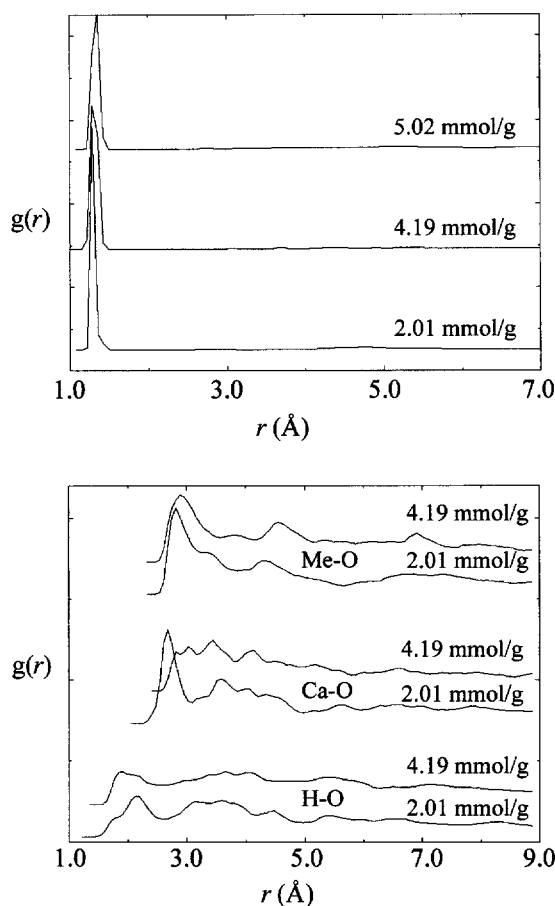


Figure 6. (Upper) Na-O radial distribution functions [$g(r)$] for solvent contents of 2.01, 4.19 and 5.02 mmol/g. O denotes the oxygen atom of the methanol. (Lower) H-O, Na-O and Me-O $g(r)$ functions for solvent contents of 2.01 and 4.19 mmol/g. O, Me and H represent the oxygen atoms of the framework, the methyl groups and the hydrogen atoms of the methanol molecule, respectively. All of the $g(r)$ functions were evaluated by averaging on the configurations related to the final 50,000 steps of the expansion run in the ensemble $N\sigma T$.

ecules involves an energetic minimum to a methanol content of 4.2 mmol/g, when the filling process of the first layer is complete.

CONCLUSIONS

Molecular dynamics simulations were performed on Camp Berteau montmorillonite saturated with Ca^{2+} and Na^+ ions, over a wide range of methanol concentration. The force-field parameters were in part drawn from the literature (Ferrario *et al.*, 1990; Rappè *et al.*, 1992) and in part fitted to experimental data. The analysis indicated that methanol molecules in a monolayer form clusters with each Ca^{2+} and Na^+ ion linked to 4 or 2 methanol molecules, respectively. After the complete filling of the first layer, the formation of a second layer and a third layer begins and the coordination

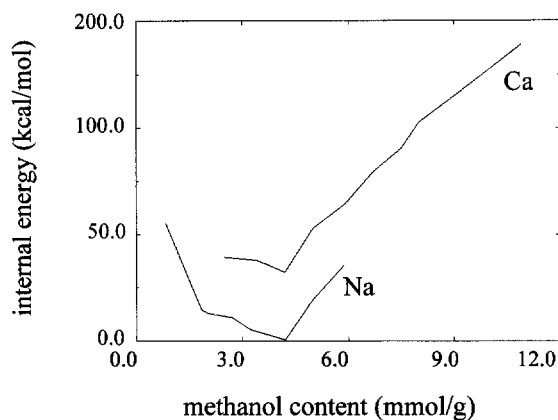


Figure 7. Relationship between the internal energy of interlayer methanol and the solvent content for Ca-rich montmorillonite and Na-rich montmorillonite systems.

sphere of the metal ions increases to 6 methanol molecules for Ca-rich montmorillonite, and 4 methanol molecules for Na-rich montmorillonite. These data are consistent with experiment. The analysis of the radial distribution functions and the computation of the self-diffusion coefficients indicates that diffusion of methanol in montmorillonites is slower than that of H_2O (Chang *et al.*, 1995). Future investigations will involve introducing H_2O molecules into the systems, and using a model with larger dimensions and an unconstrained framework. The molecular dynamics models can be further refined with more accurate calorimetric measures of the adsorption enthalpy, more reliable diffusion coefficients values, and more precise diffraction and spectroscopic experimental data.

ACKNOWLEDGMENTS

The authors gratefully acknowledge S. Guggenheim and R. Cygan for critical reading of the manuscript, and for helpful comments and suggestions. For financial support, thanks are due to MURST and CNR.

REFERENCES

- Allen, M.P. and Tildesley, D.J. (1987) *Computer Simulations of Liquids*. Clarendon Press, Oxford, England, 385 pp.
- Annabi-Bergaya, F., Cruz, M.I., Gataineau, L. and Fripiat, J.J. (1979) Adsorption of alcohols by smectites: I. Distinction between internal and external surfaces. *Clay Minerals*, **14**, 249–258.
- Annabi-Bergaya, F., Cruz, M.I., Gataineau, L. and Fripiat, J.J. (1980a) Adsorption of alcohols by smectites: II. Role of the exchange cations. *Clay Minerals*, **15**, 219–223.
- Annabi-Bergaya, F., Cruz, M.I., Gataineau, L. and Fripiat, J.J. (1980b) Adsorption of alcohols by smectites: III. Nature of the bonds. *Clay Minerals*, **15**, 225–237.
- Annabi-Bergaya, F., Cruz, M.I., Gataineau, L. and Fripiat, J.J. (1981) Adsorption of alcohols by smectites: IV. Models. *Clay Minerals*, **16**, 115–122.
- Boyd, S.A. and Mortland, M.M. (1985) Dioxin radical formation and polymerization on Cu(II)-smectite. *Nature*, **316**, 532–535.

- Chang, F.C., Skipper, N.T. and Sposito, G. (1995) Computer simulation of interlayer molecular structure in sodium montmorillonite hydrates. *Langmuir*, **11**, 2734–2741.
- Delville, A. (1993) Structure and properties of confined liquids: A molecular model of the clay-water interface. *Journal of Physical Chemistry*, **97**, 9703–9712.
- Eltantawy, I.M. and Arnold, P.W. (1974) Ethylene glycol sorption by homoionic montmorillonites. *Journal of Soil Science*, **25**, 99–110.
- Ferrario, M., Haughney, M., McDonald, I.R. and Klein, M.L. (1990) Molecular-dynamics simulation of aqueous mixtures: Methanol, acetone, and ammonia. *Journal of Chemical Physics*, **93**, 5156–5166.
- Grandjean, J. and Laszlo, P. (1989) Deuterium nuclear magnetic resonance studies of water molecules restrained by their proximity to a clay surface. *Clays and Clay Minerals*, **37**, 403–408.
- Haughney, M., Ferrario, M. and McDonald, I.R. (1987) Molecular-dynamics simulation of liquid methanol. *Journal of Physical Chemistry*, **91**, 4934–4940.
- Keldsen, G.L., Nicholas, J.B., Carrado, K.A. and Winans, R.E. (1994) Molecular modeling of the enthalpies of adsorption of hydrocarbons on smectite clay. *Journal of Physical Chemistry*, **98**, 279–284.
- Lanson, B. (1997) Decomposition of experimental X-ray diffraction patterns (profile fitting): a convenient way to study clay minerals. *Clays and Clay Minerals*, **2**, 132–146.
- Mackenzie, R.C. and Mitchell B.D. (1972) Soils. Pp. 267–298 in: *Differential Thermal Analysis*, (R.C. Mackenzie, editor). Academic Press, London.
- Pamar-Robert, A., Khirat-Bensaada, M. and Robert L. (1989) Insertion d'alcools par la montmorillonite: Étude à partir des isothermes d'adsorption composites en phase liquide. *Bulletin de la Société Chimique Française*, **5**, 579–590.
- Rappé, A.K., Casewit, C.J., Colwell, K.S., Goddard III, W.A. and Skiff, W.M. (1992) UFF, A full periodic table force field for molecular mechanics and molecular-dynamics simulations. *Journal of the American Chemical Society*, **114**, 10024–10035.
- Sato, H., Yamagishi, A., Naka, K. and Kato, S. (1996) Monte Carlo simulations on intercalation of tris(1,10-phenantroline)metal(II) by saponite clay. *Journal of Physical Chemistry*, **100**, 1711–1717.
- Skipper, N.T., Chang, F.C. and Sposito, G. (1995) Monte Carlo simulation of interlayer molecular structure in swelling clay minerals. 1. Methodology. *Clays and Clay Minerals*, **43**, 285–293.
- Smith, W. and Forester T.R. (1996) *DLPOLY is a package of molecular simulation routines*. Copyright the Council for the Central Laboratory of the Research Councils. Daresbury Laboratory, Daresbury, UK.
- Sposito, G. and Prost, R. (1982) Structure of water adsorbed on smectites. *Chemical Review*, **82**, 553–573.
- Vahedi-Faridi, A. and Guggenheim, S. (1999) Structural study of monomethylammonium and dimethylammonium-exchanged vermiculites. *Clays and Clay Minerals*, **3**, 338–347.
- Van Olphen, H. and Fripiat, J.J. (1979) *Data Handbook for Clay Materials and Other Non-Metallic Materials*. Pergamon, Oxford, England, 346 pp.
- Villemure, G., Detellier, C. and Szabo, A.G. (1986) Fluorescence of clay-intercalated methylviologen. *Journal of the American Chemical Society*, **108**, 4658–4659.

E-mail of corresponding author: marco.pintore@univ-orleans.fr

(Received 10 July 1998; revised 20 December 2000; Ms 98-092; A.E. Randall T. Cygan)